Optical Switching in VO$_2$ films by below-gap excitation

M. Rini[1], C. Giannetti[2], S. Fourmaux[3], S. Wall[4], Z. Hao[1], F. Parmigiani[2], A. Fujimori[5], M. Onoda[6], J.C. Kieffer[4], R.W. Schoenlein[1], A.Cavalleri[4]*

[1]*Materials Sciences Division Lawrence Berkeley National Laboratory.*
[2]*Dipartimento di Fisica, Universita' di Brescia. Italy*
[3]*Université du Québec, INRS énergie et matériaux, Varennes, Québec.*
[4]*Department of Physics. Clarendon Laboratory, University of Oxford, UK*
[5]*Department of Physics, University of Tokyo*
[6]*Institute of Physics, University of Tsukuba, Ibaraki, Japan*

We study the photo-induced insulator-metal transition in VO$_2$, correlating threshold and dynamic evolution with excitation wavelength. In high-quality single crystal samples, we find that switching can only be induced with photon energies above the 670-meV gap. This contrasts with the case of polycrystalline films, where formation of the metallic state can also be triggered with photon energies as low as 180 meV, well below the bandgap. Perfection of this process may be conducive to novel schemes for optical switches, limiters and detectors, operating at room temperature in the mid-IR.

Correlated electron systems are often very sensitive to external perturbations and exhibit dramatic transitions between competing structural, electronic or magnetic phases[i]. Switching of the macroscopic properties can be achieved by controlling temperature, pressure, electric[ii] or magnetic fields[iii], with potential applications that range from sensors to data storage. Optical excitation is emerging as a new tool to drive phase changes in correlated electron systems on the femtosecond timescale[iv], potentially opening new avenues to high bit-rate applications.

The photo-induced insulator-to-metal transition in VO_2 is one of such photo-control phenomena[v,vi,vii]. In its low-T phase (T_c < 340 K), VO_2 has cell-doubled monoclinic structure, derived from the high-temperature rutile phase by pairing and tilting of V^{4+} cations along the c axis. Concomitantly with this structural distortion, the V3d charge carriers localize into spin singlets on the V^{4+} dimers, causing a metal-insulator transition[viii,ix] (see figure 1). The nature of the thermally-driven phase transition has been debated for several decades[x,xi], specifically in relation to (a) the driving force that causes the dimerization and (b) the nature of the insulating state[xii].

Photo-excitation across the gap depletes the localized states in the valence band, injecting electrons into the spatially extended conduction band. As a result of such prompt *hole photo-doping*, the energy gain derived from the pairing is lost, the distortion is coherently relaxed and the metallic phase is formed. This process can also be seen as a displacive excitation of large amplitude coherent phonons[xiii,xiv,xv], where photo-injection of holes into the valence band shifts the equilibrium ionic position from the dimerized state to the high-symmetry phase.

Due to the technological potential of this process, in the past we have also investigated the response of VO$_2$ at telecom wavelengths[xvi]. We have shown how the use of nanoparticles in glass makes the ultrafast phase transition compatible with optical fiber geometries and results in an efficient room-temperature switching behavior at 1.55 microns. Other experiments have reported the use of VO$_2$ in opal-based photonic crystals as another strategy to switch optical properties of a photonic material[xvii].

Here, we report on new studies of the excitation wavelength dependence for this photo-induced phase transition, comparing the response to light tuned above and below the bandgap. The main conclusion of our work is that single crystals respond very differently from polycrystalline films. In the former, where the onset of optical absorption coincides with the bandgap, we show that no photo-induced phase transition can take place if the photon energy is below 670 meV. Thus, in single crystal samples interband optical absorption is the dominant mechanism driving the transition. On the contrary, in the thin films the insulator-metal transition can be controlled with photon energies below gap, extending to less than 180 meV. The threshold follows the linear absorption coefficient, which is significant already at low photon energies. This is presumably indicative of the importance of hole-photo-doping to drive the insulator-metal transition, which is made possible by the existence of defect states in the middle of the gap.

Figure 1 shows the temperature dependent resistivity for the single crystals and thin films. Single crystal samples were grown by chemical vapor transport[xviii], whereas thin films polycrystalline samples were grown by reactive rf-magnetron sputtering[xix]. Both samples evidence an insulator-metal transition near 340 K, with similar hysteresis curves that reflect the first-order nature of this transition. As expected, the transition region is

sharper in the single crystal than in the thin films, both upon heating and cooling. The absolute resistivity change across the insulator-metal transition is higher in the single crystal samples than in the thin films. By plotting $-\ln(1/\text{resistivity})$ as a function of $(1/2k_bT)$ in the insulating phase, one finds identical activation energy (bandgap) of 670 meV for both samples. The observation of a smaller resistivity change across the transition can likely be explained by the higher defect density of the polycrystalline films, resulting in lower carrier mobility for the metallic phase and higher intrinsic dopant densities in the insulator.

Time-dependent reflectivity and transmission were measured in the standard pump-probe geometry, performed by keeping the sample at room temperature. The femtosecond pump pulses where obtained by optical parametric conversion of 800-nm pulses from a 1 KHz, Ti:Sa amplified laser system. By exploiting signal (S) and idler (I) pulses as well as S-I difference frequency radiation in GaSe and AgGaSe, the excitation pulses were continuously tunable between 1 and 20 μm. The time-dependent optical constants were probed only at the fundamental 800-nm wavelength of the same femtosecond laser. The results are shown in figure 2. Because the 50-nm VO_2 film was thin compared to the absorption depth of both pump and probe pulses, we could directly convert our transmission measurements into the time-dependent absorption coefficient across the photo-induced insulator-metal transition. In the bulk samples, the penetration depth of the IR pump pulse was significantly larger than the 800-nm probe for all excitation wavelengths. Thus, a homogeneously excited region was probed also in the bulk samples.

In figure 3 we report the pump-fluence dependence of the differential absorption coefficient for the thin films at +300-fs time delay (qualitatively similar results were

obtained for the bulk samples). The absorbed fluence was estimated by subtracting transmitted and reflected energy from the incident pulse energy, normalizing to the excitation spot size as measured in situ with knife-edge measurements. A fluence threshold, a region of monotonic increase and a saturation value are found. We take the value of the threshold as the intercept with the zero differential change in absorption at 300 fs[xx]. The threshold for the transition is about 250 $\mu J/cm^2$, which at 1 eV corresponds to 8 10^{21} absorbed photons/cm^3, or one absorbed photon every 60 unit cells. No significant change in threshold was found for all the pump photon energies above the bandgap.

Figure 4a shows the most compelling observation of our paper, i.e. the response of the thin films to below-gap optical excitation. The fluence-dependence is the same as that for above gap excitation, although the efficiency of the process is reduced. An approximately rigid shift of the curves toward higher fluences is observed. Figure 4b summarizes these observations comparing them to the results for bulk samples. The value of the threshold is plotted as a function of pump photon energy for thin films and bulk. Strikingly, the threshold is seen to diverge much more rapidly for single crystals than for thin films.

Figure 5 displays the linear absorption coefficient for a range of wavelengths in the mid-IR for both thin films and for single-crystal samples[xxi]. The resonances near 0.1 eV correspond to IR active lattice vibrations. At higher energy the absorption is low, but grows significantly in the films already near 200 meV. Thus, irradiation in the 200 meV – 670 meV region results in significant absorption in the thin films.

While the main purpose of this paper is to report the observation of this effect, we note that this is consistent with our understanding of the photo-induced phase transition in a

Peierls (or spin Peierls) insulator. Long-wavelength excitations in the thin films of VO_2 presumably take place between the valence band and non-mobile defect states below the bandgap, resulting in effective hole photo-doping. Within this picture, it is possible to argue that the transition is driven solely by hole photo-doping, i.e. by the removal of electrons from the singlet states that stabilize the low-T phase. Thus, the nature of the final states into which the electrons are promoted, as long as these are not "binding" states for the V-V pairs, does not affect the insulator-metal transition.

In summary, we have shown that polycrystalline VO_2 films can be switched between the insulating and metallic phases by photo-absorption below the electrical bandgap. This is likely due to the existence of defect states in the middle of the gap, allowing for hole photo-doping into the valence band. Our work may be conducive to novel schemes for optical switching, limiting or sensing in the mid-IR, where the existence of defect states and mid-gap absorption can be put to good use in systems where hole photo-doping drives the insulator-metal transition.

single crystal

film

10^4

10^2

10^0

10^{-2}

10^{-4}

250

350

T [K]

10

8

6

4

2

film
$E_g = 0.67$ eV

single crystal
$E_g = 0.67$ eV

20

22

$1 / (2 k_b T)$

Figure 1

t < 0: Insulator

3d$_{//}$

3d$_{\pi}$

E$_{pump}$ = 0.76 eV

3d$_{//}$

t > 200 fs: Metal

3d$_{\pi}$

E$_f$

3d$_{//}$

Thin Films

E$_{pump}$ = 0.76 eV
E$_{probe}$ = 1.5 eV

Bulk

E$_{pump}$ = 0.76 eV
E$_{probe}$ = 1.5 eV

Delay (ps)

Delay (ps)

$\frac{\Delta\alpha}{\alpha}$

ΔR
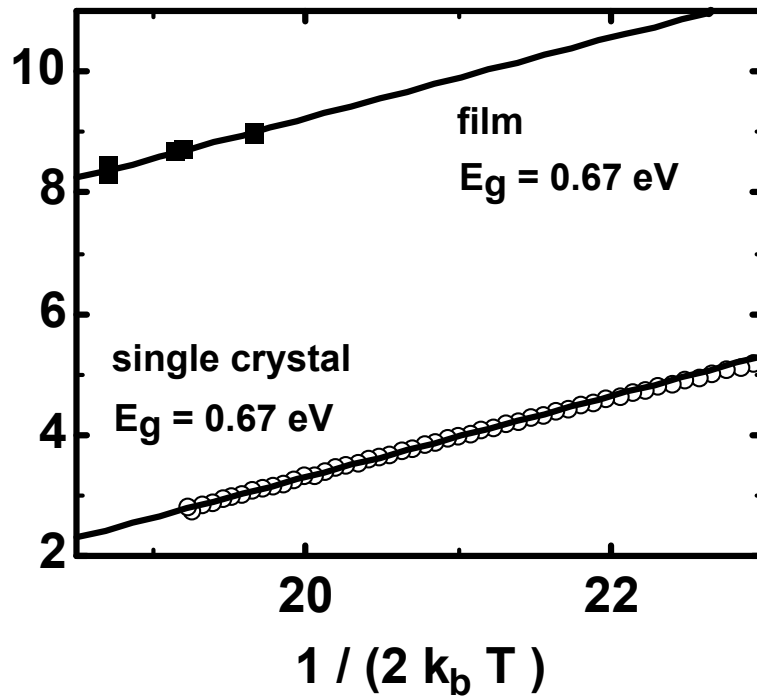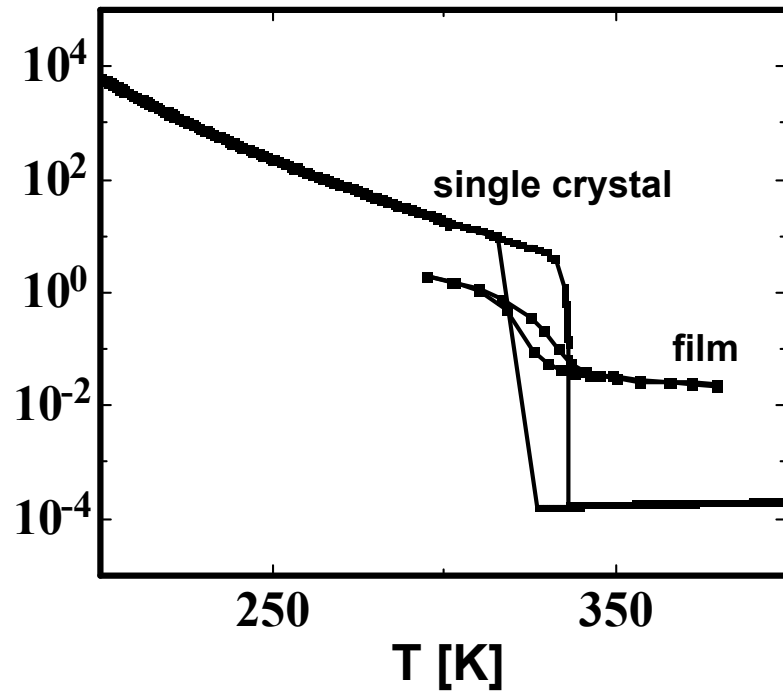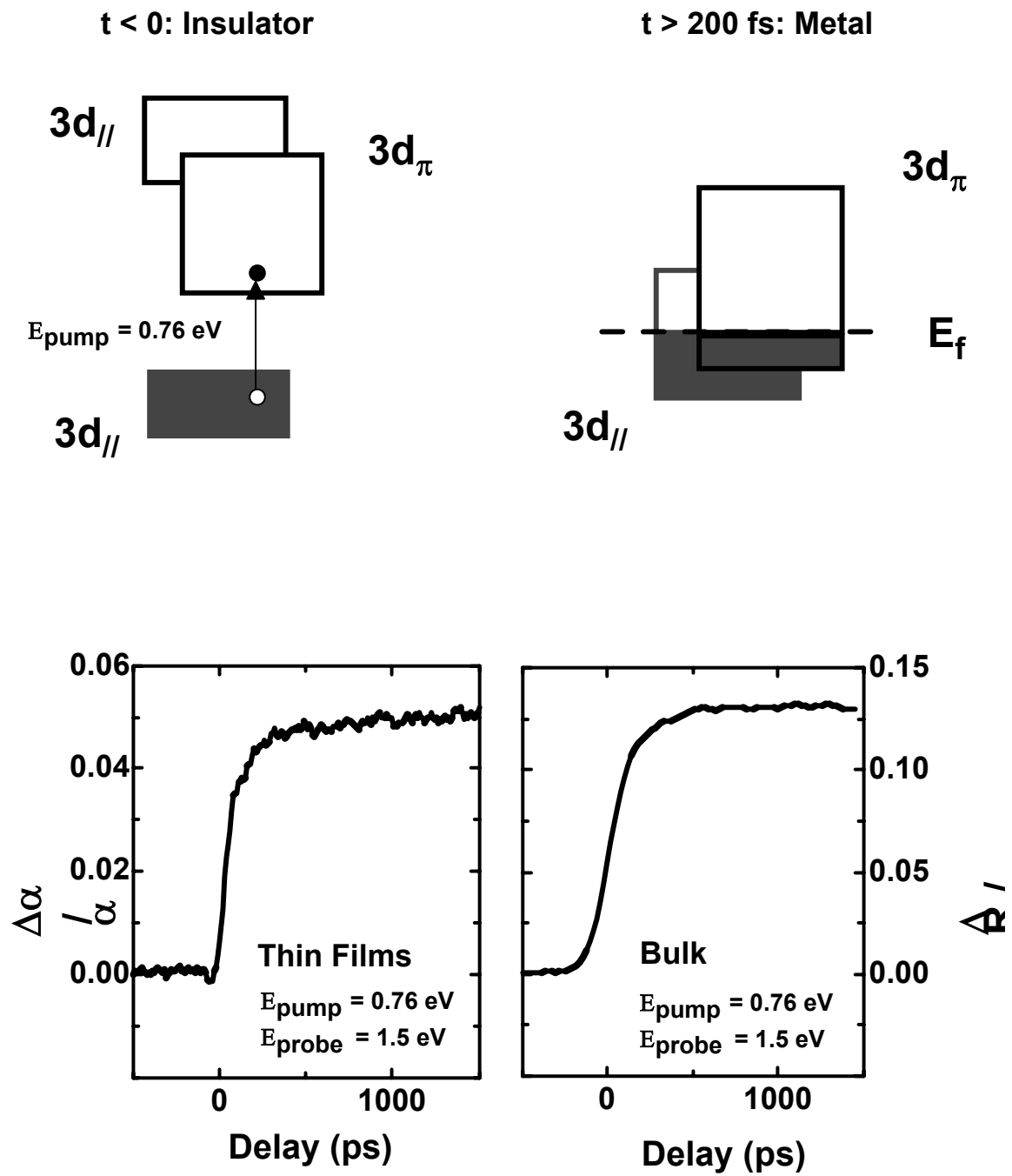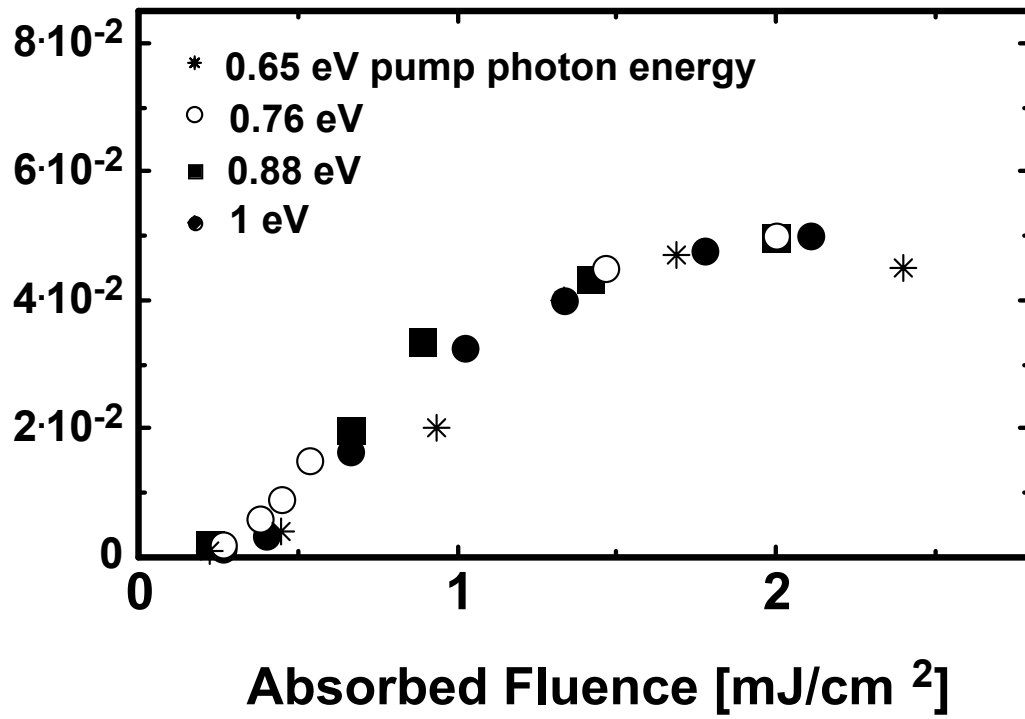
Figure 2

Figure 3

Absorbed Fluence (mJ/cm ^{2})

F_{th} (0.75 eV) F_{th} (0.54 eV) F_{th} (0.37 eV)
0.25 mJ/cm^2 0.7 mJ/cm^2 2 mJ/cm^2

Figure 4a

Figure 4b

50-nm films

2·10⁻³

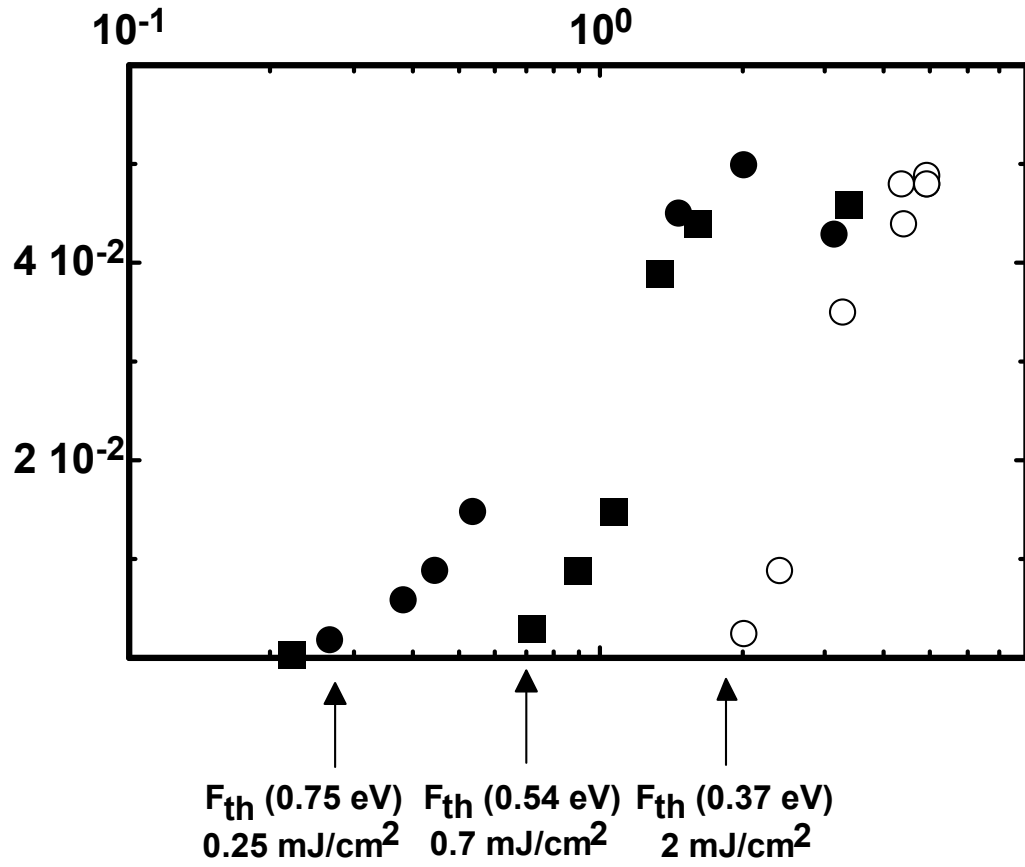**1·10⁻³**

Bulk

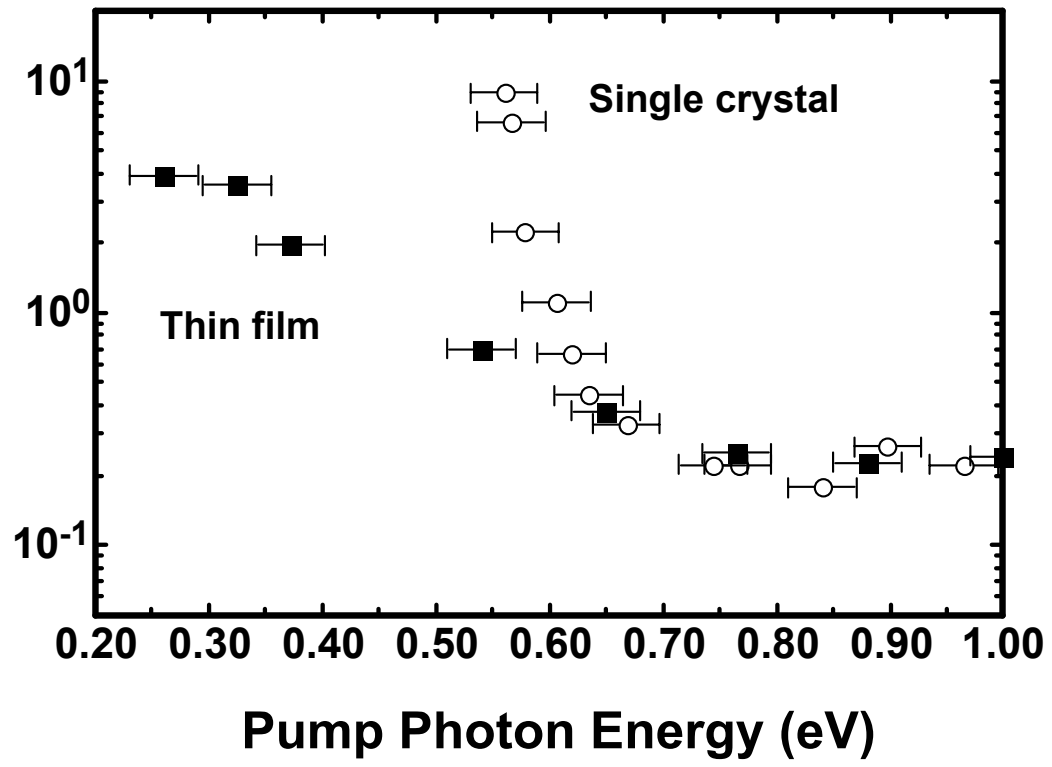**0.0　　0.2　　0.4　　0.6**
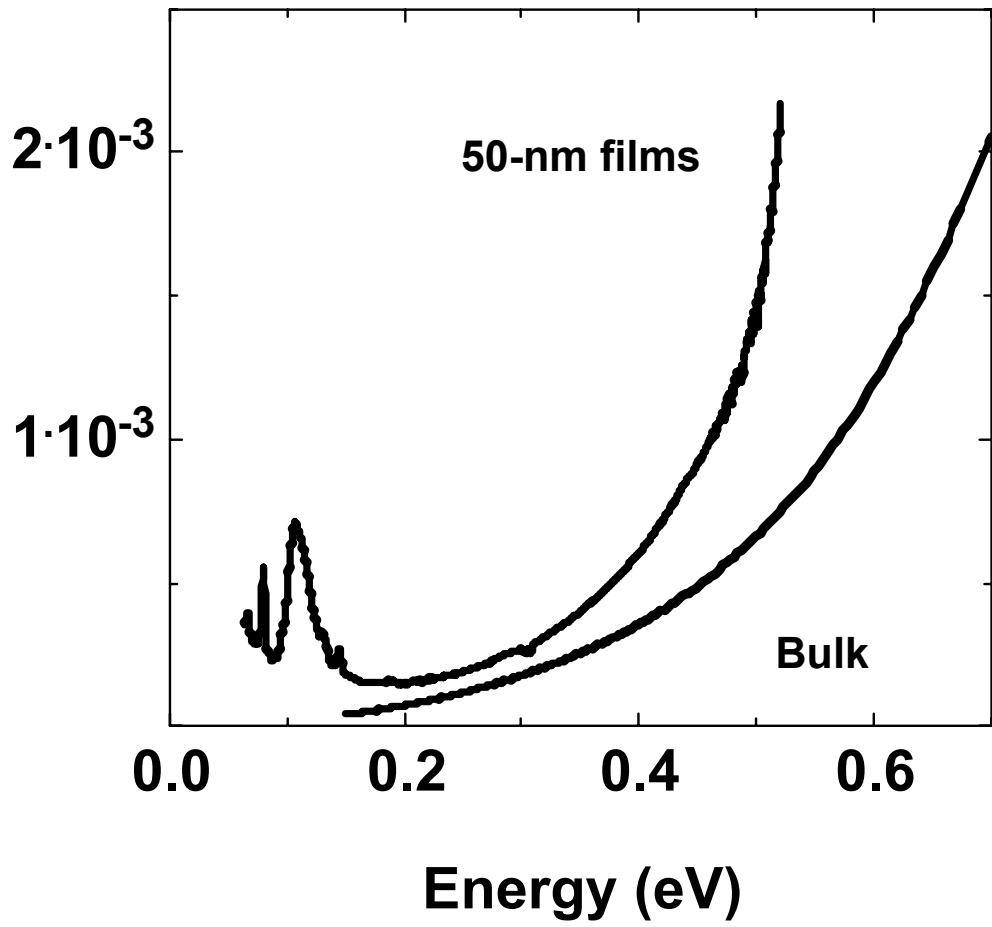
Energy (eV)

Figure 5

FIGURE CAPTIONS

Figure 1 Temperature dependent resistivity of single-crystal and thin film VO_2. The insulator-metal transition occurs in both samples near 340 K, with similar hysteresis curves. The transition region is sharper in the single crystal than in the thin films. A fit to the resistivity in the insulating phase gives an activation energy (bandgap) of 670 meV for both samples.

Figure 2 Schematic band diagram of VO_2. In the insulating phase a 0.67 eV bandgap is formed between the $3d_{//}$ valence band and the $3d_{\pi}$ conduction band. A second empty conduction band has the same 3d// symmetry as the valence band, split by a Peierls distortion and by the Hubbard energy. Photo-excitation at high photo-doping energies is dominated by $3d_{//}$ - $3d_{\pi}$ transitions, which dope holes into the valence band and cause collapse of the bandgap. Time dependent optical response of single-crystal and thin-film VO_2 after photo-excitation with 0.76-eV pulses from an optical parametric amplifier.

Figure 3 Fluence dependence of the photo-induced phase transition in the thin films for various pump photon energies above the bandgap. A threshold of 250 $\mu J/cm^2$ is found for all photon energies, with a region of super-linear growth and saturation.

Figure 4. (a) Fluence dependence of the photo-induced phase transition in the thin films for various pump photon energies below the bandgap. The response is qualitatively similar to what observed for above-bandgap excitation, although a rigid shift to the right reflects a less efficient photo-doping process. **(b)** Threshold for the photo-induced phase transition for various wavelengths in bulk and thin films. The threshold is found to diverge rapidly for the single crystal, whilst in the case of the thin films the phase transition can be induced for photon energies as low as 180 meV.

Figure 5 Measurement of the IR absorption coefficient for VO_2 thin films. Significant absorption is found immediately above 200 meV, due to transitions between the valence band and mid-gap defect states. The absorption coefficient for high quality single crystal samples (ref 24) exhibits lower absorption at photon energies below the bandgap.

REFERENCES

[i] Imada, Fujimori, Tokura *Rev. of Modern Phys.* **70**, 1039 (1998).

[ii] A. Asamitsu, Y. Tomioka, H. Kuwahara, Y. Yokura et al. *Nature* **50**, 388 (1997).

[iii] H. Yoshizawa, H. Kawano, Y. Tomioka, Y. Tokura *Phys. Rev. B* **52** R13145 (1995)

[iv] K. Myiano, T. Tanaka, Y. Tomioka, Y. Tokura *Phys. Rev. Lett.* **78**, 4257 (1997).

[v] A.Cavalleri, Cs Toth, C.W. Siders, J.A. Squier, F. Raksi, P. Forget, J.C. Kieffer *Phys. Rev. Lett.* **87**, 237401 (2001).

[vi] S. Iwai, M.Ono, A. Maeda, H. Matsuzaki, H. Kishida, H. Okamoto, Y. Tokura *Phys. Rev. Lett.* **91**, 057401 (2003).

[vii] M. Chollet, L. Guerin, N. Uchida, S. Fukaya, H. Shimoda, T. Ishikawa, K. Matsuda, T. Hasegawa, A. Ohta, H. Yamochi, G. Saito, R. Tazaki, S. Adachi, S. Koshihara, *Science* **307**, 86 (2005).

[viii] F.J. Morin *Phys. Rev. Lett.* **3**, 34 (1959).

[ix] S. Bierman et al. *Phys. Rev. Lett.* **94**, 026404 (2005).

[x] J.B. Goodenough *J. Sol. State Chem.* 3, 490 (1961).

[xi] A. Zylbersteyn and N. Mott *Phys. Rev. B.* **11**, 4383 (1975).

[xii] R.M. Wentzcovic, W.W. Schultz, P.B. Allen *Phys. Rev. Lett.* **72**, 3389 (1994).

[xiii] A. Cavalleri, T. Dekorsy, H.H.W. Chong, J.C. Kieffer, R.W. Schoenlein *Phys. Rev. B* **70**, 161102(R) (2004).

[xiv] H.J. Zeiger, J. Vidal, T.K. Cheng, E.P. Ippen, G. Dresselhaus, M.S. Dresselhaus *Phys. Rev. B* **45**, 157 (1994)

[xv] G.A. Garret, T.F. Albrecht, J.F. Whitaker, R. Merlin *Phys. Rev Lett.* **77**, 3661 (1996).

[xvi] M. Rini, A. Cavalleri, R.W. Schoenlein, R. Lopez, T.E. Haynes, R.F. Haglund, L.A. Boatner, L.C. Feldman, *Opt. Lett.* **30**, 558 (2005).

[xvii] D. Mazurenko et al. *Appl. Phys. Lett.* **86**, 041114 (2005)

[xviii] V_2O_3 powders were first prepared by heating V_2O_5 at 973 K for 24 hours. Next, polycrystalline samples were grown by heating a mixture of V_2O_3 and V_2O_5 at 1173 K for 24 hours in nitrogen atmosphere. Resultant polycrystalline samples and $TeCl_4$ were sealed in a quarts tube, of which the high temperature part was 1323 K and the low temperature part was 1173 K. The result of the thermogravimetric analysis (TGA) was VO {2.002\pm0.0002}. The lattice constants at room temperature were a =5.764 Å, b = 4.539 Å, c = 5.393 Å and beta = 122.61 degrees.

[xix] A >99.9% pure vanadium target was used for the sputtering, which was performed in an argon and oxygen gas mixture at an operating pressure better than 10 mTorr, and deposited onto Si (100) substrate previously coated with 200 nm low-pressure-vapor-deposited amorphous Si_3N_4 layer. The 50 nm film thickness was measured ex situ by cross sectional scanning electron (SEM) observations. The samples were etched to have free-standing 50-nm/200-nm VO_2/Si_3N_4 structures. The films were also characterized by measuring X-ray diffraction, X-ray absorption[xix] spectra and Raman scattering, which showed the same characteristics of pure VO_2 powders.

[xx] J.M. Liu *Opt. Lett.* **7**, 196 (1982)

[xxi] Hans W. Verleur, A. S. Barker, Jr., and C. N. Berglund, *Phys. Rev.* **172**, 788 (1968)